Reforming Antenna Engineering Pedagogy: 1D-to-2D Monopole Teaching Using Gain-to-Length Ratio and Circular Disc Monopole Demonstrations at 433 MHz for Improved Learning Outcomes in Higher Education

Jinfeng Li, *Member, IAENG* and Haolin Zhou

***Abstract*—Conventional teaching of omnidirectional monopole antennas relies on image theory but often lacks interpretability regarding the engineering merits of the quarter-wave principle. This study bridges the gaps among fundamental physics, applied research, and higher education by introducing a novel comprehensive performance metric—the Gain-over-Length Ratio (GoLR)—defined specifically for the antenna's radiating element. Furthermore, we extend prior work by numerically investigating the two-dimensional (2D) shaping effects on vertical monopole configurations operating at 433 MHz, a sub-gigahertz frequency widely used in low-earth orbit (LEO) satellite tracking. Under identical grounding conditions, the GoLR is employed to comprehensively evaluate and compare an optimised 1D vertical monopole and an optimised 2D circular disc monopole (CDM). Two new observations are derived and highlighted in this work. First, the CDM antenna rejects the conventional quarter-wave conjecture for the perimeter. Instead, it is the height (diameter) of the CDM that really matters, not the perimeter. Second, the CDM design exhibits a smeared GoLR profile as a function of height (diameter) compared to the 1D monopole, leading to a marginally more compact vertical profile, specifically, a 0.85 cm reduction in height relative to the 1D counterpart. However, this dimensional optimisation comes at a slight cost: a GoLR reduction of 0.04012 dBi/cm. The insights derived from this work—integrating teaching methodologies and engineering applications—mark a significant step toward fostering student-led antenna innovations tailored for industry-collaborative, purpose-driven applications.**

***Index Terms*—antenna education, circular disc monopole, antenna gain, engineering pedagogy, engineering physics, microwave engineering, monopole antenna, higher education, radiation efficiency, 433 MHz**

Manuscript received April 18, 2025; revised June 20, 2025.

This work was supported by the National Natural Science Foundation of China under Grant 62301043, and the Fundamental Research Funds for the Central Universities (Beijing Institute of Technology Research Fund Programme for Young Scholars) under Grant 220502052024011.

Jinfeng Li is an assistant professor of the Beijing Key Laboratory of Millimeter Wave and Terahertz Technology, School of Interdisciplinary Science, Beijing Institute of Technology, Beijing, 100081, China (corresponding author, e-mail: jinfengcambridge@bit.edu.cn).

Haolin Zhou is a postgraduate research student of the Beijing Key Laboratory of Millimeter Wave and Terahertz Technology, School of Integrated Circuits and Electronics, Beijing Institute of Technology, Beijing, 100081, China (email: zhouhaolin@bit.edu.cn).

I. Introduction

ANTENNA technology [1–5] teaching in higher education—particularly within microwave engineering [6–8] curricula—must integrate not only fundamental theory [9] and mathematical foundations [10] but also practical implementation [11] under real-world constraints [12]. Effective pedagogical delivery requires holistic curriculum design, active student engagement [13], and comparative assessment [14] within the broader radiofrequency (RF) engineering framework. For instance, while the ground-based monopole paradigm [15] is widely recognised for its simplicity and compactness compared to the dipole (both operating on resonance principles), its practical implementation demands further footprint minimisation [16][17] without significantly degrading antenna gain [18][19] (as mathematically illustrated in Fig. 1). This optimisation is critical to meet the increasingly stringent demands of 5G (fifth generation) [20] and post-5G [21] wireless systems.

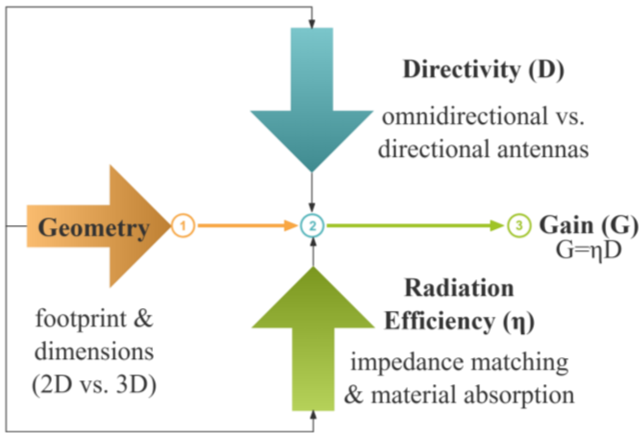

Fig. 1. Key teaching (and design) essentials of monopole antennas, featuring three-pronged approach involving geometry and footprint, directivity (D) and radiating efficiency (η), and ultimately, the comprehensive metric of gain (G).

Among the modalities listed in Fig. 1, the directivity (D) of a monopole antenna, a measure of how effectively the antenna radiates in a specific direction compared to an isotropic source, is inherently linked to the monopole length, the configuration of the ground plane, and the operational frequency. For a monopole over a perfect ground plane (where the image theory works perfectly), the directivity (D) can be analytically approximated as Eq. (1) in a spherical coordinate with azimuthal angle θ ranging from 0 to 2π, and the zenith angle φ from 0 to π. The measure of directivity physically represents a dimensionless ratio of the peak normalized radiation pattern intensity (in a specific direction, i.e., the main beam) over the average radiation pattern (i.e., among all directions of the field detachment from the antenna into the space, more specifically, in the far field regime):

$$D = \frac{4\pi}{\int_0^{2\pi}\int_0^{\pi} U(\theta,\varphi)\sin\theta d\theta d\varphi}, \quad (1)$$

where $U(\theta,\varphi)$ represents the radiation intensity in the direction of (θ,φ). In an ideal case, a quarter-wavelength monopole exhibits its strongest radiation in the horizontal plane (azimuth), perpendicular to the monopole, with diminishing intensity along the vertical axis (dead zone). In real-world implementations, however, directivity is influenced by practical considerations, e.g., the variability in radial lengths [12], environmental factors, and fabrication tolerances [22][23]. The relationship between these parameters and the antenna's directivity (D) demonstrates a multidimensional dependency, requiring systematic exploration and optimisation.

Radiation efficiency (η) is a power quantification (relative to the input power) after being degraded by the antenna material's absorption and the reflection losses prior to the radiating action (i.e., the field before detachment of the antenna). For a vertical monopole (i.e., a single straight conductor mounted over a conductive ground plane) and the 2D disc monopole (same vertical setup but with a diverse radiator shape), no dielectric materials are used, i.e., only metal (ohmic) loss is consumed. With the same conductor material used (e.g., copper) for different geometry designs, impedance matching (and mismatching) arguably dictates the radiation efficiency (η) of the monopole.

Conventionally, as observed in the mainstream microwave engineering lecture notes, the η is directly given in relation to the forward reflection coefficient S_{11}. There are two-fold concerns about the status. First, the use of the scattering parameters (e.g., S_{11}) usually overlooks the specification of the linear scale or logarithmic scale (dB), which can be misleading to not only students, but also experienced engineers and academics. Second, the intermediate steps for deriving the mathematical relationship between η and S_{11} are missing. In this context, we derive this in detail from Eq. (2) to Eq. (9) below, for the sake of boosting both educational and engineering physics understanding into this subject matter. Here the radiated power is denoted as P_{rad}, the reflected power is denoted as $P_{reflect}$, the material absorption is denoted as P_a. Note that P_a is zero for perfect electric conductors utilized in this work for constructing monopole antennas (no dielectrics are used). The linear scale of the reflection coefficient is represented by $|S_{11}|_{linear}$, and its more usual decibel (dB) scale is denoted as S_{11} (dB).

$$\eta = \frac{P_{rad}}{P_{in}} = \frac{P_{rad}}{P_{loss}+P_{rad}}, \quad (2)$$

$$P_{loss} = P_{reflect} + P_a, \quad (3)$$

$$\eta = \frac{P_{rad}}{P_{reflect}+P_{rad}}, \quad (4)$$

$$S_{11}\,(dB) = 10\log\left(\frac{P_{reflect}}{P_{reflect}+P_{rad}}\right) = 20\log|S_{11}|_{linear}, \quad (5)$$

$$\frac{P_{reflect}}{P_{reflect}+P_{rad}} + \frac{P_{rad}}{P_{reflect}+P_{rad}} = 1, \quad (6)$$

$$\eta = \frac{P_{rad}}{P_{reflect}+P_{rad}} = 1 - \frac{P_{reflect}}{P_{reflect}+P_{rad}}, \quad (7)$$

$$\frac{P_{reflect}}{P_{reflect}+P_{rad}} = |S_{11}|_{linear}^{\;2} = 10^{\frac{S_{11}\,(dB)}{10}}, \quad (8)$$

$$\eta = 1 - |S_{11}|_{linear}^{\;2} = 1 - 10^{\frac{S_{11}\,(dB)}{10}}. \quad (9)$$

In this regard, the antenna gain (G), defined as G=ηD as per Fig. 1, is arguably dictated by the impedance-matching [24] or mismatching [25] status and the directivity (D) [15] of the vertical monopole designs (valid for both 1D and 2D). Based on these assumptions (theoretically valid), explorative learning and engineering demonstration-based teaching of quarter-wave monopole antennas in higher-education (Beijing Institute of Technology) is carried out jointly in an undergraduate elective module entitled States of the Arts in Liquid Crystals Millimeter-wave Technology for 6G (run in 2024), as well as a third-year undergraduate compulsory module entitled Frontiers and Progress of Electrical and Computer Engineering in 2025 from February to April.

By introducing a new Gain-over-Length-Ratio (GoLR) concept, mimicking the figure-of-merit [26][27] in other engineering sectors, students and nonspecialists can develop a transferable understanding of the comprehensive performance and footprint trade-off among different antenna structures. The engineering insights newly built up in this work complement the conventionally taught classical physics-based solutions (image theory), and march toward a complete (unified) science-based solution to the key antenna paradigm (i.e. monopole) that underpins wide-ranging application fields.

II. Rejection of Perimeter Conjecture for CDM

Since monopole (1D vertical radiator) and its variation of CDM (2D vertical radiator) are resonant-based antennas, the 1D monopole's principle of relying on current distributions along its length (odd multiples of a quarter wavelength) for efficient radiation is reasonably transferable to the study into CDM (2D vertical radiator) in this section.

Diving into the optimally designed CDM involves a few steps for students-led explorative learning. First, a reasonable Perimeter Conjecture on the CDM is assigned for dedicated students to validate, i.e., we deduce that the CDM antenna functions similarly (length effect) by the perimeter equaling a quarter-wavelength (i.e., an initial conjecture as depicted in Fig. 2), inferring the diameter of 5.17 cm for the CDM by design.

With this myth in mind, students carry out a series of MATLAB simulations, signal processing, and results analysis with a hands-on guide drawn from the modelling practice documented and published for a vertical monopole antenna with the same tool [12][15]. The sub-GHz ISM band 433 MHz (license-free) is taken as an example, serving various real-world scenarios, e.g., LoRa [28] and walkie-talkies [29].

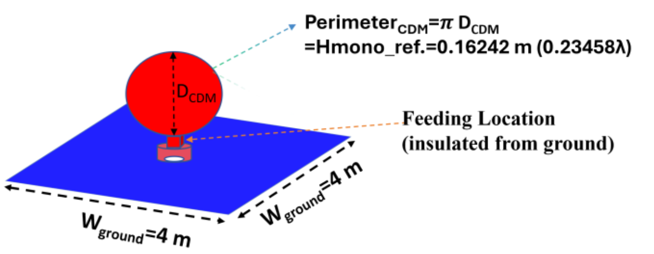

Fig. 2. Design conjecture based on vertical CDM's perimeter equaling the vertical quarter-wavelength monopole's height.

Accordingly, the scattering parameter (forward reflection coefficient S_{11}) is quantified by parameterising the designed diameter of the CDM's radiator for evaluating the impedance matching. Arguably, the quarter-wave Perimeter Conjecture serves a counterexample on the impedance match (i.e., highly mismatched), as evidenced in Fig. 3 for the return loss result of 0.08727 dB (i.e., almost all the input power is reflected) for the CDM's diameter design of 5.17 cm (corresponding to the Perimeter Conjecture of monopole) at 433 MHz.

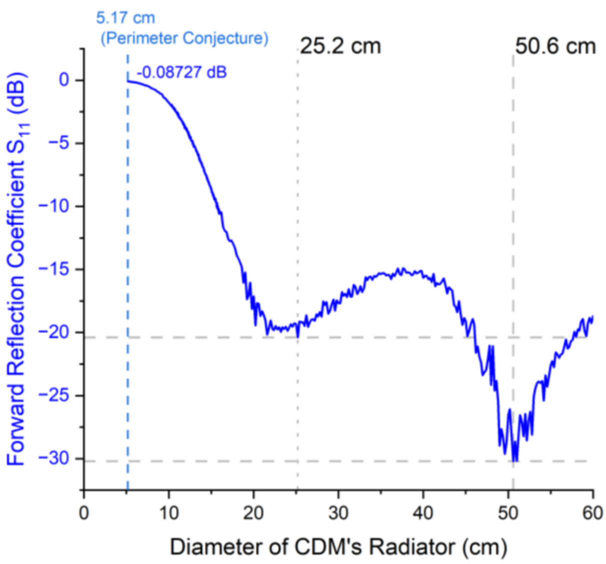

Fig. 3. MATLAB simulation results of forward reflection coefficient at 433 MHz for Circular Disc Monopole (CDM) antennas with unified ground size of 4 m by 4 m (5.77 wavelengths) and the diameter parameterised from 5.17 cm (perimeter of 0.23458 wavelengths at 433 MHz, i.e., corresponding to the quarter-wave Perimeter Conjecture of monopole) to 60 cm (perimeter of 2.72242 wavelengths at 433 MHz).

The impedance matching status improves (i.e., return loss reduces) with the increase of the CDM radiator's diameter to 25.2 cm (i.e., its perimeter corresponding to 1.14342 wavelengths), with a return loss of 20.38337 dB reported in Fig. 3. Afterwards, the increase of the diameter leads to fluctuations in S_{11}, with the optimal impedance-matching diameter observed at 50.6 cm (i.e., the perimeter corresponding to 2.29591 wavelengths), with the return loss dropping to 30.20624 dB for this design at 433 MHz. To evaluate the wider band performance of the three cases discussed, Figure 4 captures the frequency response of the reflection coefficients, compared among the three designs mentioned across the spectrum from 390 MHz to 476 MHz, i.e., ±10% of the central frequency of 433 MHz.

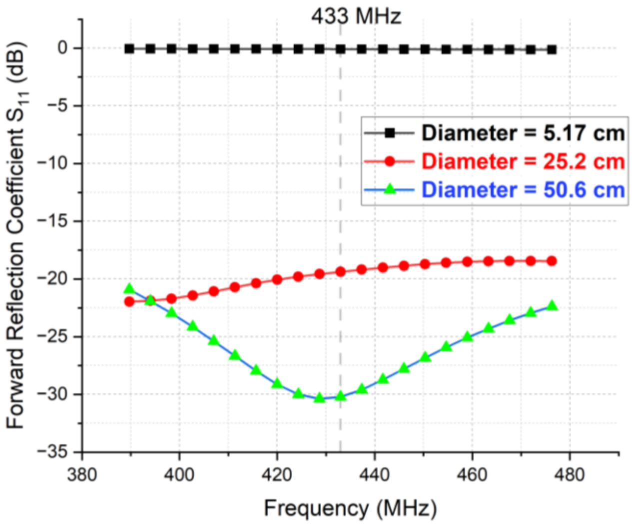

Fig. 4. MATLAB simulation results of forward reflection coefficient across 390 MHz to 476 MHz for Circular Disc Monopole (CDM) antennas with a unified ground size of 4 m by 4 m (5.77 wavelengths) and different diameters of the radiator.

On the same space parameterisation range as per Fig. 2 for the CDM radiator's diameter, the directivity results of the antenna (derived from the 3D radiation pattern) are obtained in Fig. 5. Notably, the diameter under the Perimeter Conjecture gives a maximum directivity of 6.05548 dBi. The increase of the diameter from this boundary to the 33 cm witnesses an increase of the maximum directivity to 6.82379 dBi (occurring when the perimeter reaches 1.49733 wavelengths at 433 MHz). Interestingly, for the further increase in the diameter, there is a slump in the directivity to 5.27226 dBi (for the diameter of 44.4 cm, corresponding to the perimeter of 2.01459 wavelengths at 433 MHz).

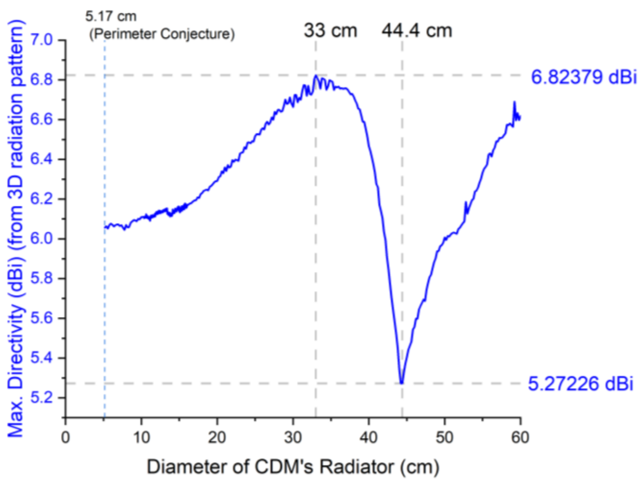

Fig. 5. MATLAB simulation results of maximum directivity at 433 MHz for Circular Disc Monopole (CDM) antennas with unified ground size of 4 m by 4 m (5.77 wavelengths) and the diameter parameterised from 5.17 cm (perimeter of 0.23458 wavelengths at 433 MHz, i.e., corresponding to the quarter-wave Perimeter Conjecture of monopole) to 60 cm (perimeter of 2.72242 wavelengths at 433 MHz).

As per equations (2)−(9), the radiation efficiency is analytically derived for the CDM designs with the radiator's diameter parameterised from the same range as per Fig. 5, i.e., from 5.17 cm to 60 cm. The results are benchmarked and justified with those obtained by MATLAB simulation as shown in Fig. 6, i.e., agreement between theoretical and simulated results is well evidenced. Notably, there is an extremely low (nearly zero) radiation efficiency for the Perimeter Conjecture case (diameter of 5.17 cm), indicating a total reflection as analysed before in Fig. 3. With the rise in the diameter, radiation efficiency starts increasing. When the CDM's diameter of the radiator rises to 19.2 cm (perimeter corresponding to 0.87117 wavelength), the radiation efficiency starts levelling off at 98.162%. A comprehensive results presentation is graphed in Fig. 7, involving the radiation efficiency and the return loss together for ease of understanding. In summary, the results reject the presence of the quarter-wave-based Perimeter Conjecture for the CDM.

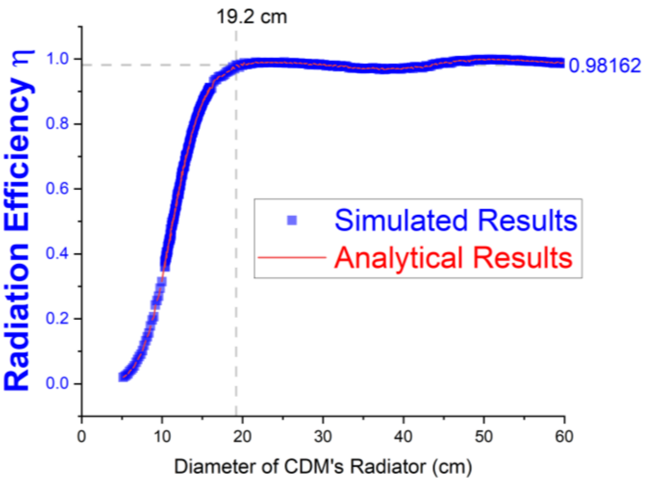

Fig. 6. MATLAB simulation results vs. analytical results of radiation efficiency at 433 MHz for Circular Disc Monopole (CDM) antennas with unified ground size of 4 m by 4 m (5.77 wavelengths) and the diameter parameterised from 5.17 cm (perimeter of 0.23458 wavelengths at 433 MHz, i.e., corresponding to the quarter-wave Perimeter Conjecture of monopole) to 60 cm (perimeter of 2.72242 wavelengths at 433 MHz).

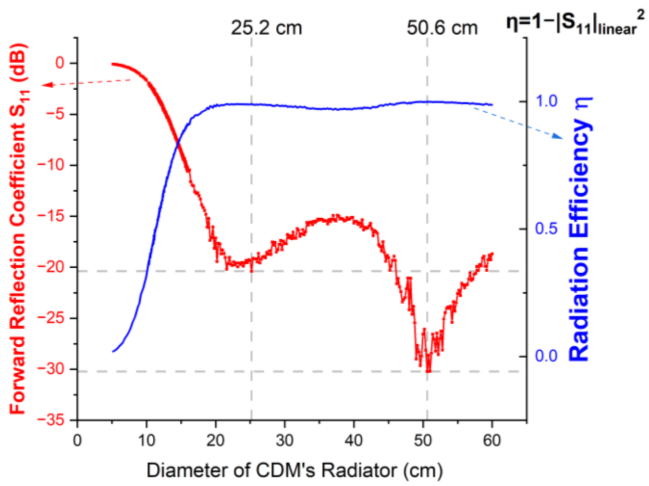

Fig. 7. MATLAB simulation results of return loss (left axis) and radiation efficiency (right axis) at 433 MHz for Circular Disc Monopole (CDM) antennas with unified ground size of 4 m by 4 m (5.77 wavelengths) and the diameter parameterised from 5.17 cm (perimeter of 0.23458 wavelengths at 433 MHz, i.e., corresponding to the quarter-wave Perimeter Conjecture of monopole) to 60 cm (perimeter of 2.72242 wavelengths at 433 MHz).

III. 2D CDM VS. 1D MONOPOLE AND PROPOSAL OF GOLR

Summarising the results from last section and comprehending the impedance-mismatched quarter-wave Perimeter Conjecture (rejection for use) further, a generalised parameterisation of the radiator's height is conducted for both the CDM and the vertical monopole, in the format of D_{CDM} (diameter of the CDM's radiator, instead of the perimeter) for the CDM, and H_{mono} for the length or height of the 1D vertical monopole, as per Fig. 8, i.e., both antennas are with a unified ground size of 4 m by 4 m (5.77 wavelengths) and the diameter (height) parameterised from 5.17 cm (perimeter of 0.23458 wavelengths at 433 MHz, i.e., corresponding to the Perimeter Conjecture of monopole) to 60 cm (perimeter of 2.72242 wavelengths at 433 MHz).

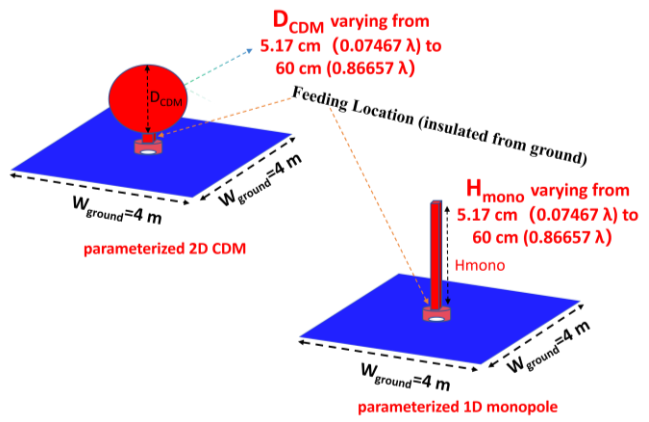

Fig. 8. Comparative parameterisation study of vertical monopole (1D) with vertical CDM (2D) in the vertical plane. The same grounding material and geometry (4 m by 4 m) are assumed for both designs.

A. Gain and GoLR Parameterised with Diameter of CDM

The comprehensive radiation metric of gain (G) is obtained by multiplying the radiation efficiency (η) by the directivity (D) as obtained earlier. From the results shown in Fig. 9, the gain (G) largely follows the trend of radiation efficiency (as quantified and discussed in Fig. 7).

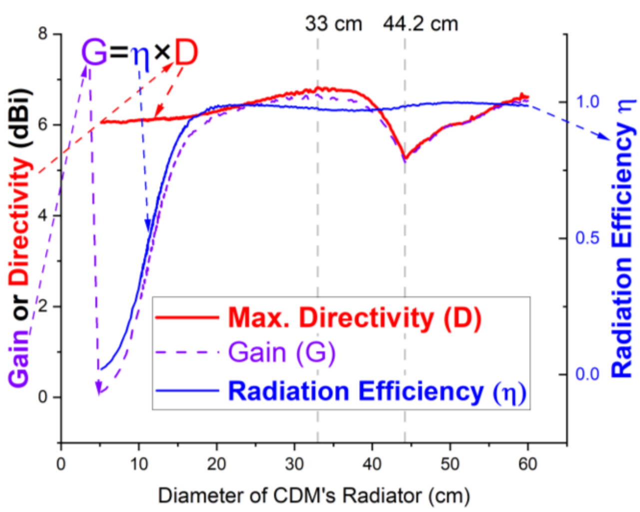

Fig. 9. MATLAB simulation results of gain and directivity (left axis) and radiation efficiency (right axis) at 433 MHz for Circular Disc Monopole (CDM) antennas with unified ground size of 4 m by 4 m (5.77 wavelengths) and the diameter parameterised from 5.17 cm (perimeter of 0.23458 wavelengths at 433 MHz, i.e., corresponding to the Perimeter Conjecture of monopole) to 60 cm (perimeter of 2.72242 wavelengths at 433 MHz).

To be more specific, gain reaches the maximum at CDM's radiator diameter of 33 cm, i.e., further increase of the diameter results in no enhancement but a decline of the gain, as illustrated in a local minimum of radiation efficiency as well as the gain at the radiator's diameter of 44.2 cm. To comprehensively capture this geometry-wise performance impact, the gain-over-diameter-ratio (GoDR) is proposed in this work, by taking the ratio of the antenna gain (G) over the diameter of the CDM's radiator here. The results are depicted in Fig. 10, wherein the maximal GoDR of the CDM (0.35572 dBi/cm) occurs at the CDM radiator's diameter of 15.32 cm (0.22127 wavelength), i.e., slightly shorter (lowered-profile) than the 1D quarter-wave monopole benchmark with a referenced height of 16.27 cm (0.2349 wavelength) [12][15] at 433 MHz.

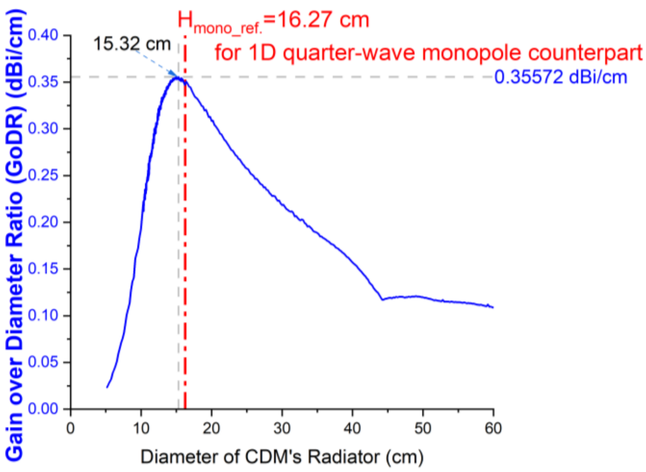

Fig. 10. MATLAB simulation results of gain-over-diameter-ratio (GoDR in dBi per cm) at 433 MHz for Circular Disc Monopole (CDM) antennas with a unified ground size of 4 m by 4 m (5.77 wavelengths) and the diameter parameterised from 5.17 cm (perimeter of 0.23458 wavelengths at 433 MHz, i.e., corresponding to the Perimeter Conjecture of monopole) to 60 cm (perimeter of 2.72242 wavelengths at 433 MHz).

B. *Parameterised Radiator's Height of 1D Monopole*

Interestingly, MATLAB simulation results on the 1D vertical monopole as a benchmark are reported in this section. A similar calculation procedure (parameterisation of the vertical scale from 5.17 cm to 60 cm, corresponding to 0.07467 wavelength to 0.86657 wavelength at 433 MHz) is actioned for the 1D vertical monopole (classic design). The cross-sectional size of the monopole's radiator is with a width of 0.6923 cm, corresponding to 0.0099 wavelength at 433 MHz. Note that the governing numerical method adopted in MATLAB is Method of Moments (MoM) [30].

The reflection coefficient S_{11} and the corresponding radiation efficiency η presented in Fig. 11 exhibit two dips for low return loss, and two peaks for high radiation efficiency in the radiator's height scanning range, respectively. To be more specific, the first impedance-matching point happens at the radiator's height of 16.58 cm (0.23946 wavelength), agreeing with the classic quarter-wave theorem. The second impedance-matching point occurs at 50.88 cm (0.73486 wavelength, i.e., approximated to three-quarter wavelength, the phenomenon of which well agrees with the quarter-wave theorem as well.

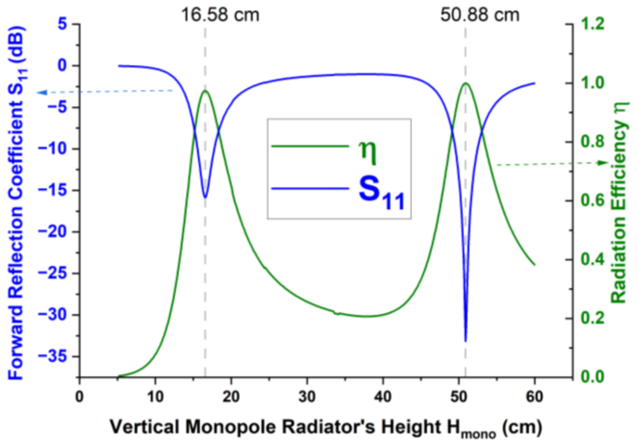

Fig. 11. MATLAB simulation results of return loss and radiation efficiency at 433 MHz for 1D vertical Monopole antennas with a unified ground size of 4 m by 4 m (5.77 wavelengths) and the radiator's height parameterised from 5.17 cm (0.07467 wavelength) to 60 cm (0.86657 wavelength) at 433 MHz.

Accordingly, the directivity and gain are obtained in Fig. 12, and the GoLR is quantified for the 1D vertical monopole in Fig. 13.

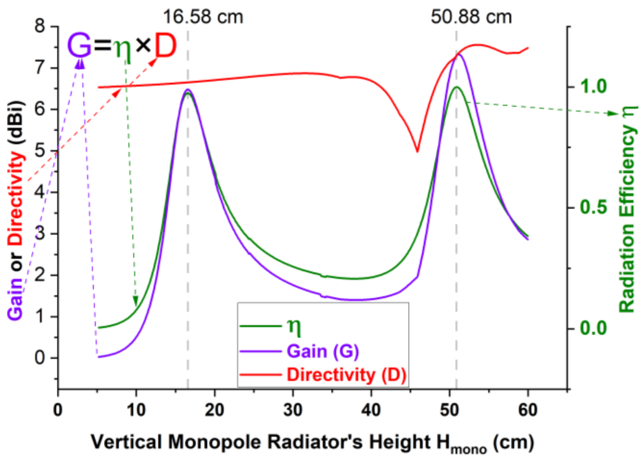

Fig. 12. MATLAB simulation results of gain and directivity (left axis) and radiation efficiency (right axis) at 433 MHz for 1D vertical Monopole antennas with unified ground size of 4 m by 4 m (5.77 wavelengths) and the radiator's height parameterised from 5.17 cm (0.07467 wavelength) to 60 cm (0.86657 wavelength) at 433 MHz.

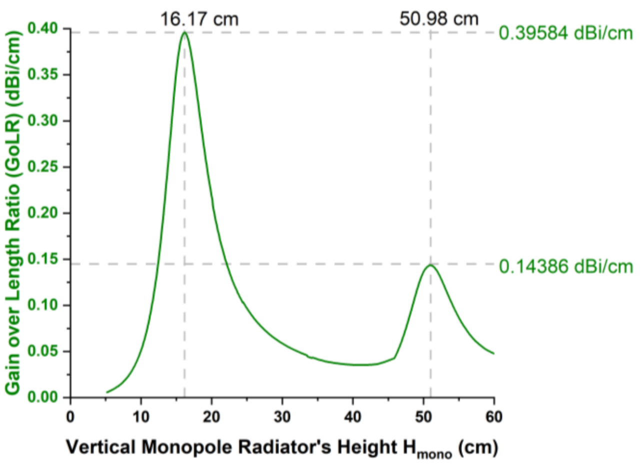

Fig. 13. MATLAB simulation results of gain-over-length-ratio (GoLR in dBi per cm) at 433 MHz for 1D vertical Monopole antennas with a unified ground size of 4 m by 4 m (5.77 wavelengths) and the radiator's height parameterised from 5.17 cm (0.07467 wavelength) to 60 cm (0.86657 wavelength) at 433 MHz.

Similarly to the CDM case, the trend of G follows closely with radiation efficiency. The geometry with the maximum GoLR of 0.39584 dBi/cm occurs at the radiator's height of 16.17 cm (corresponding to 0.23354 wavelength, i.e., near the quarter-wavelength), while the second optimum GoLR of 0.14386 dBi/cm happens at the monopole height of 50.98 cm (i.e., three-quarter wavelength). This convincingly explains the benefit of designing a quarter-wavelength one for both compact and decent performance in antenna gain.

C. Optimised 2D CDM vs. Optimised 1D Monopole

The generalised metric, gain-over-length-ratio (GoLR) is formulated and adopted for benchmarking between the 2D CDM and the 1D monopole antennas. For the 2D CDM, the GoLR is equivalent to the results obtained earlier on GoDR (gain-over-diameter-ratio), wherein the diameter equals the length for the vertical projection. The two topologies under comparison are presented in Fig. 14, with the optimal geometry sizes denoted for the CDM and 1D monopole, respectively. The results of GoLR comparison between the CDM and the 1D monopole antennas are presented in Fig. 15.

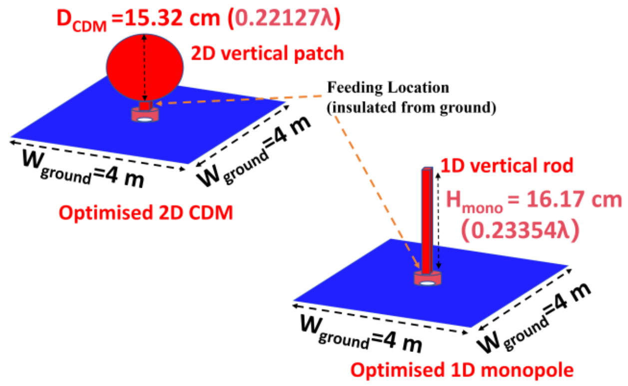

Fig. 14. Overarching comparison between the optimised 1D monopole (vertical, bottom right in the figure) and the optimised 2D CDM design model (top left in the figure). The same grounding material and geometry (4 m by 4 m) are assumed for both designs.

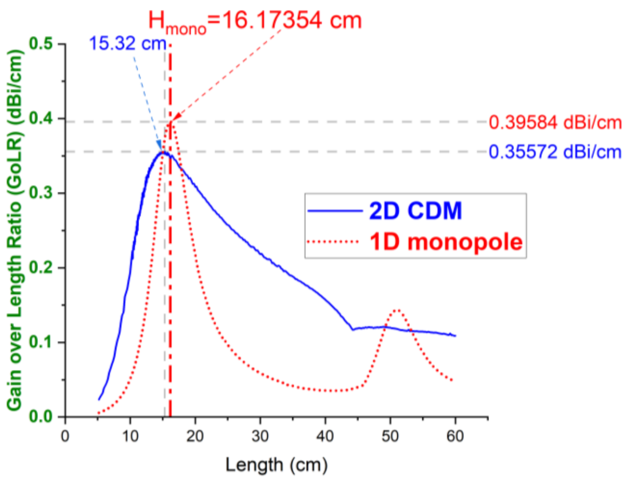

Fig. 15. MATLAB simulation results of gain-over-length-ratio (GoLR in dBi per cm) at 433 MHz for 1D vertical Monopole antennas vs. 2D CDM with unified ground size of 4 m by 4 m (5.77 wavelengths) and the radiator's height (diameter) parameterised from 5.17 cm (0.07467 wavelength) to 60 cm (0.86657 wavelength) at 433 MHz. Smearing effect of GoLR vs. antenna size (diameter) of the 2D CDM is observed.

In the current phase of this work, both the 2D CDM and 1D vertical monopole (classic) antennas demonstrate consistent observations on the benefits of one-quarter-wave operation. Interestingly, the optimum GoLR of the 2D CDM is 0.35572 dBi/cm, which happens at the critical length of 15.32 cm (0.22127 wavelength). The 1D vertical monopole design reports a slightly higher GoLR (maximum value) of 0.39584 dBi/cm occurring at the critical length of 16.17 cm (corresponding to 0.23354 wavelength).

In other words, the 2D CDM antenna design arguably presents a smeared profile of the GoLR vs. length when compared to the 1D monopole counterpart. This smearing effect leads to a slightly compact design on the height (i.e., the 2D CDM with a lower profile by 0.85 cm compared with the 1D monopole), albeit at the cost of a minor degradation of 0.04012 dBi/cm in the GoLR of interest.

Note that the footprint saving of 0.85 cm (5.55% of the 2D CDM antenna's height) as obtained at 433 MHz (ultrahigh frequency band) can lead to a substantial difference (contribution in miniaturisation) for antennas operating at extremely low frequency (ELF) and very low frequency (VLF) spectra (from 3 Hz to 30 kHz), the wavelength of which ranges from 10 km to 100000 km. The transferable size reduction can be predicted in a range from 138.75 m to 1387.5 km.

Even for a monopole antenna for Medium-wave Broadcasting service, the height reduction (if actioning the CDM design) can be significant in the urban deployment for aesthetic considerations, by way of illustration, a 639 kHz broadcasting medium wave antenna (tower) as picturized in Fig. 16. The quarter-wavelength of 117.37 m in height (operated in air) could be reduced to 110.86 m as per the CDM's smearing implication on GoLR.

Fig. 16. Photograph of a 200 kW medium-wave 639 kHz antenna in Fangshan District, Beijing for broadcasting radio signals over long distances.

IV. Discussions and Future Educational Scopes on Monopole Configuration Upgrade for Unconventional Applications

Akin to the phase-shift-to-insertion-loss ratio, indexed as figure-of-merit (FoM) and widely employed in phase-tunable RF devices [31], the GoLR index newly proposed in this work arguably corroborates the quarter-wave principle of the monopole antenna for the most effective radiation in a compact manner. From the lens of GoLR (i.e., aiming for high gain and compactness at the same time), the proof-of-principle CDM in this work is slightly less performant than its predecessor, i.e., the 433 MHz vertical quarter-wave monopole as reported in [15]. However, the CDM reaches its optimum GoLR at a slightly smaller size (0.22127 wavelength) than the monopole one (0.23354 wavelength), i.e., it has its merit of reducing the height of the antenna (albeit not significant), i.e., towards low-profile operations (albeit not yet eligible for competing with ultra-low-profile PCB counterparts, e.g., patch antennas). In addition to the antenna directivity, impedance matching, radiating efficiency, gain, gain-over-length ratio (GoLR) and radiation pattern that have been quantified in this work, bandwidth coverage and manufacturability will be assessed in future work for producing well-executed designs.

Arguably, operating as a resonant antenna, the monopole was developed a hundred years ago, with its usage spanning the general field of wireless communications and sensing. Staying updated on this mature technology through its long existence, we seek to expand the boundary by proposing an engineered index comprehending the gain and size of the antenna, i.e., gain-over-length ratio (GoLR), and apply this figure-of-merit ratio to an educational study into 433 MHz monopole antennas.

More specifically, actioning on converting vertical monopole antennas from 1D (rod) to 2D (plane), this work conducts an educational investigation into the teaching practice of circular disc monopole (CDM) benchmarked with the traditional vertical monopole, using the new index of GoLR for the integration into antenna workflows.

Building on these findings, future research shall explore new frontiers in 2D vertical monopole antenna design, e.g., by investigating the use of diverse conformal shaping for the radial-attached surfaces, including scenarios where radials are suspended in the air or affixed to non-metallic substrates. Figure 17 illustrates a typical radial rod-based discrete grounding configuration. Interestingly, the radial rods can be designed for installation and dismounting with ease, i.e., they can be bent, folded or stretched when installed for diverse environments and be conformal to diverse surfaces.

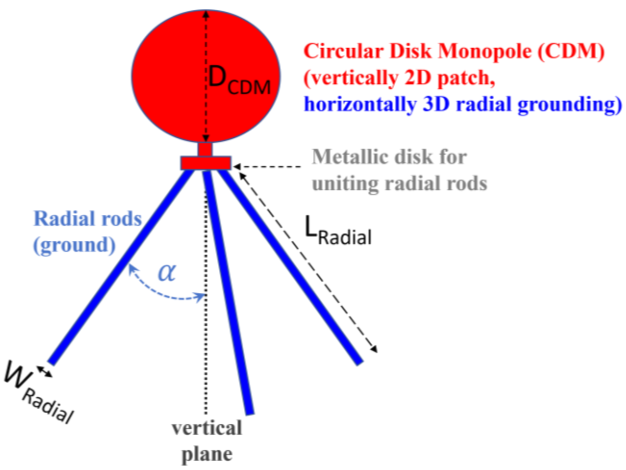

Fig. 17. Future work underway on a perturbing radial rods-based discrete grounding configuration that exemplifies its practicality in real-life applications where continuous grounding is unavailable. Scales are pictured for illustration only.

Furthermore, the radiator itself can also be made flexible and conformal to open a new door for modern applications including unconventional locations with curved edges (e.g., the interior of a submarine). Note that the submarine demands low-frequency underwater communication hardware [32] (instead of the modern high-frequency GHz communication like 4G/5G) to mitigate the significant attenuation due to sea water [33]. The early availability of 433 MHz CDM as reported in this work is envisaged to provide a custom antenna solution for maritime applications, particularly underwater communications in this regard.

Successful implementation of the GoLR concept is anticipated for low-cost low-profile installation of the quarter-wave antenna in the studied CDM topology. Application-specific scenarios for the CDM radial antenna, e.g., its potential integration into surface acoustic wave (SAW) sensing systems and in-body antennas [34][35] will be exploited. These systems often require antennas to operate on non-metallic surfaces, eliminating the need for a large continuous grounding plane typical of standard monopole designs. Multi-scale multi-physics [36–38] characterisation (with higher-order modes' prediction capability [39]) will be conducted.

Additionally, various conductive materials (not limited to copper as simulated in the current work) will be tested numerically to evaluate their impact on the CDM antenna performance. Notably, metal meshes [40][41], and transparent conductive films [42] (optically transparent and virtually invisible to the human eye) are of both research and education interest in the pursuit of various energy-efficient antenna scenarios towards a green future.

Last but not least, physical layer security-related concerns [43][44] are gaining significant attention on the roadmap to 6G communications [45][46], wherein various growing threats on hardware-based attacking scenarios [43] and software-level attacking vulnerabilities [47][48] shall be involved in the front-end components design and system integration. For the CDM device raised in this work, grounding plane attacks pose a particularly severe risk (e.g., destroying the ground plane partially or fully). Such attacks—whether involving partial or complete destruction of the ground plane—can catastrophically impair antenna functionality, translating to the loss of beam tracking in safety-critical communication and sensing applications, including autonomous vehicle communications and high-precision sensing. The resultant catastrophic beam tracking failure can lead to service disruption or even hazardous operational conditions.

To mitigate these risks, future research should explore resilient antenna designs with redundant grounding structures, real-time fault detection mechanisms, and adaptive beamforming algorithms capable of compensating for hardware degradation. Additionally, the integration of physical-layer authentication and hardware-intrinsic security features [46][50] could further safeguard CDM systems against tampering and malicious interference. As 6G networks aim to support ultra-reliable low-latency communication and mission-critical applications, addressing these security challenges at the hardware level will be imperative to ensure system robustness and user safety.

REFERENCES

[1] Cullen A, "A Source-Book of Microwave Engineering," Nature, vol. 201, no. 4924, pp1062-1062, 1964.
[2] Muttair K, Shareef O, and Taher H, "A Compact MIMO Antenna with High Efficiency for 6G Communications," Engineering Letters, vol. 33, no. 4, pp934-941, 2025.
[3] Tubbal F, Matekovits L, and Raad R, "Antenna Designs for 5G/IoT and Space Applications, 2nd Edition," Electronics, vol. 14, no. 7, pp1308-1311, 2025.
[4] Ordonez J, Vásquez L, and Pesantez P, "AntennaEDU: a novel approach for teaching and learning antenna design," Proceedings of the 2023 IEEE Colombian Caribbean Conference, pp1-6, 2023.
[5] Lim E, Wang Z, Lei C, Wang Y, and Man K, "Ultra Wideband Antennas - Past and Present," IAENG International Journal of Computer Science, vol. 37, no. 3, pp304-314, 2010.
[6] Pozar D, "Microwave engineering education: From field theory to circuit theory," Proceedings of the 2012 IEEE/MTT-S International Microwave Symposium Digest, pp1-3, 2012.
[7] Zoubi A, "Student active learning tool for producing open resources in microwave engineering education," International Journal of Engineering Pedagogy, vol. 9, no. 4, pp86-100, 2019.
[8] Gupta M, "The Role of CAD Training in Microwave Education [Educator's Corner]," IEEE Microwave Magazine, vol. 22, no. 5, pp116-120, 2021.
[9] Balanis C, "Antenna theory: a review," Proceedings of the IEEE, vol. 80, no. 1, pp7-23, 1992.
[10] Li J, Li H, Xiao Y, Jiang P, Wang S, and Guo Z, "Generalization of Impedance Characterization Methods for Liquid Crystal-Embedded Tunable Transmission Lines and Applied Study into Guard Band Redundancy Evaluation," Engineering Letters, vol. 33, no. 2, pp374-381, 2025.
[11] Popela M, Olivová J, Plíva Z, Petržílka L, Krchová M, Joska Z, and Janů P, "A Novel Approach to the Production of Printed Patch Antennas," Applied Sciences, vol. 14, no. 4, pp1556-1570, 2024.
[12] Li J, and Zhou H, "Impact of Radial Grounding Model Granularity on Directivity of 433 MHz Monopole Antennas with Flat and Inclined Radials for ISM IoT Applications," Annals of Emerging Technologies in Computing (AETiC), vol. 9, no. 1, pp44-57, 2025.
[13] Zoubi A, "Flipping the Microwave Engineering Class," Proceedings of the International Conference on Interactive Collaborative Learning, pp 809-819, 2023.
[14] Beemt A, MacLeod M, Veen J, Ven A, Baalen S, Klaassen R, and Boon M, "Interdisciplinary engineering education: A review of vision, teaching, and support," Journal of Engineering Education, vol. 109, no. 3, pp508-555, 2020.
[15] Li J, "Performance Limits of 433 MHz Quarter-wave Monopole Antennas due to Grounding Dimension and Conductivity," Annals of Emerging Technologies in Computing (AETiC), vol. 6, no. 3, pp1-10, 2022.
[16] Kabalan A, Tarot A, and Sharaiha A, "Miniaturization of a broadband monopole antenna using low loss magneto-dielectric materials in VHF band," Proceedings of the Loughborough Antennas & Propagation Conference (LAPC 2017), pp1-4, 2017.
[17] Pandey D, Sharma M, Talwar R, and Pandey B, "A compact quintuple band miniaturized elliptical planar monopole antenna for 5G/6G wireless systems," Analog Integrated Circuits and Signal Processing, vol. 122, no. 33, pp1-16, 2025.
[18] Noor S, Jusoh M, Sabapathy T, Rambe A, Vettikalladi H, Albishi A, and Himdi M, "A Patch Antenna with Enhanced Gain and Bandwidth for Sub-6 GHz and Sub-7 GHz 5G Wireless Applications," Electronics, vol. 12, no. 12, pp2555-2567, 2023.
[19] Li J, "Demystifying Two-Dimensional Asymmetrical Grounding Impacts on Monopole Antennas at 433 MHz," Proceedings of the 9th IEEE International Conference on Microwaves, Communications, Antennas, Biomedical Engineering and Electronic Systems (IEEE COMCAS 2024), pp1-4, 2024.
[20] Nakamura S, Sano M, Kuse R, and Fukusako T, "Design of a Magneto-Electric Monopole Antenna," Proceedings of the 2024 International Symposium on Antennas and Propagation (ISAP), pp1-2, 2024.
[21] Dash S, Psomas C, and Krikidis I, "Selection of metallic liquid in sub-6 GHz antenna design for 6G networks," Scientific Reports, vol. 13, no. 20551, pp1-8, 2023.
[22] Li J, "Performance Limits of Liquid Crystals Coplanar Phase Shifters beyond 60 GHz due to Fabrication," Proceedings of the IEEE International Conference on Computing, Networking, Telecommunications & Engineering Sciences Applications 2020 (IEEE CoNTESA), pp21-26, 2020.
[23] Li J, "Towards Fabrication of High-tuning-range Liquid Crystals High-aspect-ratio Coplanar Waveguide Phase Shifter by LIGA, DRIE and Laser Ablation," Proceedings of the 2023 Cross Strait Radio Science and Wireless Technology Conference (CSRSWTC 2023), pp 1-3, 2024.
[24] Li J, "Wideband PCB-to-Connectors Impedance Adapters for Liquid Crystal-Based Low-Loss Phase Shifters," Proceedings of the 50th European Microwave Conference (EuMC), pp546-549, 2021.
[25] Li J, and Li H, "Reconceiving Impedance Matching and Mismatching to Mitigate Bias-Drift in Insertion Loss of Liquid Crystal Phase Delay Lines," Photonics Letters of Poland, vol. 17, no. 1, pp35-37, 2025.
[26] Li J, and Li H, "Liquid Crystal-Filled 60 GHz Coaxially Structured Phase Shifter Design and Simulation with Enhanced Figure of Merit by Novel Permittivity-Dependent Impedance Matching," Electronics, vol. 13, no. 3, pp626-647, 2024.
[27] Li J, "Rethinking Figure-of-Merits of Liquid Crystals Shielded Coplanar Waveguide Phase Shifters at 60 GHz," J, vol. 4, no. 3, pp444-451, 2021.
[28] Hardie M, and Hoyle D, "Underground Wireless Data Transmission Using 433-MHz LoRa for Agriculture," Sensors, vol. 19, no. 19, pp4232-4249, 2019.
[29] Baker B, Woods J, Reed M, and Afford M, "A Survey of Short-Range Wireless Communication for Ultra-Low-Power Embedded Systems," Journal of Low Power Electronics and Applications, vol. 14, no. 2, pp27-46, 2024.
[30] Sefer A, Uslu M, and Sevgi L, "MATLAB-Based 3-D MoM and FDTD Codes for the RCS Analysis of Realistic Objects [Testing Ourselves]," EEE Antennas and Propagation Magazine, vol. 57, no. 4, pp122-148, 2015.
[31] Li J, "All-optically Controlled Microwave Analog Phase Shifter with Insertion Losses Balancing," Engineering Letters, vol. 28, no. 3, pp663-667, 2020.
[32] Li J, and Li H, "Passive-active crosstalk beyond low-frequency breakdown in mathematical-physical models of liquid crystal phase shifters at low-frequency applications," IET Conference Proceedings, vol. 2024, no. 30, pp592-596, 2025.
[33] Li J, and Li H, "Susceptibility to Low-Frequency Breakdown in Full-Wave Models of Liquid Crystal-Coaxially-Filled Noise-Shielded Analog Phase Shifters," Electronics, vol. 13, no. 23, pp4792-4812, 2024.
[34] Lim E, Wang J, Wang Z, Tillo T, and Man K, "The UHF Band In-body Antennas for Wireless Capsule Endoscopy," Engineering Letters, vol. 21, no. 2, pp72-80, 2013.
[35] Kamel Y, Mohamed H, ELsadek H, ELhennawy H, "RF communication between dual band implantable and on body antennas for biotelemetry application," Scientific Reports, vol. 15, no. 4065, pp1-11, 2025.
[36] Li J, "Will 'Liquid-Crystal-Based Floating-Electrode-Free Coplanar Waveguide Phase Shifter With an Additional Liquid-Crystal Layer for 28-GHz Applications' Work?" Engineering Letters, vol. 31, no. 2, pp 820-824, 2023.
[37] Li J, and Li H, "Tackling Differential Phase Shift Peaking and Degradation of Liquid Crystal Integrated Delay Line Phase Shifters with Barrel Plated Shut Micro-vias Across 1 GHz to 67 GHz," Engineering Letters, vol. 33, no. 5, pp1684-1692, 2025.
[38] Li J, and Xiao Y, "180° Differential Phase Shifting of 60 GHz Signals Using Liquid Crystal-filled Strip-Line Designs with Enhanced FoM Performance and Compact Footprint," Proceedings of the 2025 IEEE 27th International Conference on Digital Signal Processing and its Applications (DSPA), pp1-5, 2025.
[39] Li H, and Li J, "Advancing Microscale Electromagnetic Simulations for Liquid Crystal Terahertz Phase Shifters: A Diagnostic Framework for Higher-Order Mode Analysis in Closed-Source Simulators," Micro, vol. 5, no. 1, pp3-21, 2025.
[40] Abbasi M, Aziz A, AlJaloud K, et al., "Design and optimization of a transparent and flexible MIMO antenna for compact IoT and 5G applications," Scientific Reports, vol. 13, no. 20620, pp1-11, 2023.
[41] Sepat N, Sharma V, Singh D, Makhija G, and Sachdev K, "Nature-inspired bilayer metal mesh for transparent conducting electrode application," Materials Letters, vol. 232, no. 2018, pp95-98, 2018.
[42] Elsokary A, Soliman M, Abulfotuh F, Ebrahim S, Shafai T, and Karim M, "Fabrication of composite transparent conductive electrodes based on silver nanowires," Scientific Reports, vol. 14, no. 3045, pp1-15, 2024.
[43] Li J, and Li H, "Dielectric Leakage Attacks on Liquid Crystal Phase Shifters in 60 GHz WiGig Systems," Electronics Letters, vol. 61, no. 1, pp70317-70321, 2025.
[44] Li J, "Optically Inspired Cryptography and Cryptanalysis: A Survey and Research Directions," Lecture Notes of the Institute for Computer

Sciences, Social Informatics and Telecommunications Engineering (LNICST), vol. 332, no. 2020, pp98-110, 2020.
[45] Bhide P, Shetty D, and Mikkili S, "Review on 6G communication and its architecture, technologies included, challenges, security challenges and requirements, applications, with respect to AI domain," IET Quantum Communication, vol. 6, no. 1, pp12114-12136, 2024.
[46] Li J, and Li H, "Harnessing Liquid Crystals-based Techniques for Unleashing 6G Network Security Paradigms," Engineering Letters, vol. 33, no. 6, pp2027-2036, 2025.
[47] Li J, and Li H, "Evolution of Application Security based on OWASP Top 10 and CWE/SANS Top 25 with Predictions for the 2025 OWASP Top 10," Proceedings of the IEEE 8th International Conference on Inventive Computation Technologies (ICICT 2025), pp1178-1183, 2025.
[48] Li J, "Vulnerabilities Mapping based on OWASP-SANS: A Survey for Static Application Security Testing (SAST)," Annals of Emerging Technologies in Computing (AETiC), vol. 4, no. 3, pp1-8, 2020.
[49] Jornet J, Knightly E, and Mittleman D, "Wireless communications sensing and security above 100 GHz," Nature Communications, vol. 14, no.841, pp1-10, 2023.
[50] Kamal M, Abideen S, Sharafian A, Ibrahim A, Islam M, and Habib S, "Securing Communication Networks at the Physical Layer: A DRL and Phase Optimization Approach," IET Signal Processing, vol. 2025, no. 1, pp6422115-6422125, 2025.

Jinfeng Li (M'20) is a microwave engineer, a specialist in novel reconfigurable RF devices, as well as an authority on liquid crystals-based microwave and millimeter-wave technology. He received the B.Eng. degree (1st class) in electrical and electronics engineering from the University of Birmingham and Huazhong University of Science & Technology, in 2013, the MPhil degree in nuclear energy from the University of Cambridge, in 2014, and the Ph.D. degree in liquid crystals microwave and millimeter-wave electronics engineering from the University of Cambridge, in 2019.

From 2019, he joined the University of Southampton as a research fellow, Imperial College London as a visiting research fellow, and Nuclear Futures Institute (Bangor University) as a research associate. He is currently an Assistant Professor with Beijing Key Laboratory of Millimeter Wave and Terahertz Technology, School of Integrated Circuits and Electronics, as well as the Advanced Research Institute of Multidisciplinary Science at Beijing Institute of Technology. In the past ten years, his research experiences include (1) microwave and millimeter-wave beam steering and tunable devices based on liquid crystals for 5G/6G, inter-satellite communications, and radio astronomical instrumentation; (2) wireless surface acoustic wave sensors antenna array for monitoring the structural integrity of LNG tanks; (3) light water reactor thermal hydraulics facility and instrumentation development in North Wales; (4) optical fiber based multi-phase flow characterisation; (5) computational modelling of nuclear reactor core using Monte Carlo and deterministic methods for nuclear energy policy decision-making; (6) motor drives of multilevel multicell inverters for fuel economy and sustainable cities; (7) application security and sentiment analysis of big data for stock market forecasting; (8) contact tracing and health informatics for COVID-19 (cited by PNAS and Lancet Public Health). He has edited three books, authored or co-authored over 80 journal articles and conference papers.

Prof. Li was a recipient of the IET Award, the AP Jarvis Prize (highest final-year-project honor in University of Birmingham), the AETiC Highly Cited Article Award 2023, and three Best Paper Awards at IEEE, IOP and IET conferences, respectively. He was a Cambridge Trust Scholar, Speaker at IEEE AP-S/URSI 2024 and the 50th & 46th European Microwave Conferences, Emerging Technologist with Barclays UK, Editorial Board member of three Science Citation Index journals, TPC and Session Chair of seven IEEE conferences, including IEEE ISAP (27th International Symposium on Antennas and Propagation), IEEE 15th International Conference on Microwave and Millimeter Wave Technology (ICMMT 2023), IEEE/IFAC 10th International Conference on Control, Decision and Information Technologies (CoDIT 2024), IEEE COINS 2024, IEEE VCC 2024, IEEE SNAMS 2019, and 5th China and International Young Scientist Terahertz Conference etc. He was elected Senior Member of the China Institute of Communications (CIC), Top 1% Reviewer on Publons (Web of Science), Reviewing Expert for the China Academic Degrees and Graduate Education Development Center, Grants Reviewer for the National Natural Science Foundation of China (NSFC), Newton Prize (£1m fund) reviewer for the UK National Commission for UNESCO, and Grants Reviewer for the Health and Social Care Delivery Research (HSDR) fund from National Institute for Health Research (NIHR), UK.

Prof. Li is also an award-winning Concert Pianist and Composer with over 20 piano recitals across China and the UK (2004 - now), including Central Hall Westminster, Princess Alexandra Hall, London Guildhall, Royal Academy of Music the Duke's Hall, Cambridge Corn Exchange, West Road Concert Hall, Wuhan Qintai Concert Hall etc. He is a Concert Pianist for Hughes Hall and Wolfson College, University of Cambridge. His representative works of original piano music include: The Last-Minute Flight, Parity Non-conservation, Silicon-based Life, Room-temperature Superconductivity, Solar Storm, Quantum Entanglement, etc. Prof. Li was elected National-level Young Talent in 2023. He teaches four undergraduate modules including (1) States of the Arts in Liquid Crystals Millimeter-wave Technology for 6G; (2) Frontiers and Progress of Electrical and Computer Engineering; (3) States of the Arts in Piano; and (4) Frontiers of Electronic Science and Technology. He and his student won the Best Paper Award at IET GEn-CITy 2024.

Haolin Zhou is pursuing a postgraduate degree in microwave and terahertz engineering at Beijing Institute of Technology under the supervision of Prof. Jinfeng Li who leads the Liquid Crystal Millimeter-wave Technology Group. His current research activity centres upon the use of Method of Moments (MoM) and other state-of-the-art computational techniques for precisely characterising radiofrequency components and devices (including but not limited to antennas, and other wired and wireless devices), to understand the performance limits and identify the knowledge gaps both physically and numerically.